IAC-25,B2,IPB,17,x9948

QUBE Mission Update: First Year of Operation of a 3U CubeSat for Quantum-Key-Distribution Experiments

Timon Petermann®a*, Lisa Elsner®a, Benedikt Schmidta, Dominik Pearson®a, Tanuja Datara, Ilham Mammadova, Eric Jägera, Chaitnya Chopraa, Malavika Unnikrishnana, Johannes Dauner®a, Vijay Nagalingesha, Markus Kraussa, Roland Habera, Klaus Schilling®a, Benjamin Rödiger®b, René Rüddenklau®b, Ömer Bayraktar®c,d, Jonas Pudelkoc,d, Joost Vermeerc,d, Christoph Marquardt®c,d, Michael Auer®e, Adomas Baliuka®e, Moritz Birkholde, Peter Freiwang®e, Michael Steinberger®e, Wenjamin Rosenfeld®e, Harald Weinfurter®e, Lukas Knips®e

Abstract

Satellite-based quantum key distribution (QKD) is crucial for global secure communication, yet its implementation on compact platforms remains a technical challenge. The QUBE mission is a technology demonstrator for satellite-based QKD aspects, integrating three payloads - a quantum random number generator and two transmitters for polarization and phase-encoded quantum states, respectively - into a 3U CubeSat. These are complemented by the optical space infrared downlink system for QUBE (OSIRIS4QUBE) to enable optical transmission of the generated quantum states. One of the core challenges of the mission was maintaining subdegree pointing precision to the optical ground station (OGS) in conjunction with dynamic optical signal acquisition and tracking. Following its launch on 16 August 2024, QUBE completed a rigorous commissioning phase and entered full operational mode. This paper presents operational insights and results from its first year in orbit. We detail results from attitude determination and control system (ADCS) tests - actuator verification, detumbling, sensor calibration, and fine-pointing mode evaluation - critical for experiment operations. Notably, QUBE successfully achieved autonomous optical downlink establishment with stable links over complete overpasses and reliable sub-degree pointing error, validating its capability for the quantum state transmission. The complexity of the mission revealed key lessons in system integration, operations & autonomy, and link reliability offering valuable guidance for the design and execution of future low-cost, scalable satellite QKD deployments.

Acronyms		FAU	Friedrich-Alexander-Universität
ADCS	attitude determination and control system		Erlangen-Nürnberg
COMMS	communication subsystem	FSM	fine steering mirror
CPF	consolidated prediction format	GDS	generic data system
DLR	German Aerospace Center	GNSS	global navigation satellite system
EM	engineering model	GSN	ground station network
EPS	electrical power system	IGRF	international geomagnetic reference field
LIS	ciccurcui power system	LCT	laser communication terminal

IAC-25,B2,IPB,17,x9948 Page 1 of 16

^a Zentrum für Telematik (ZfT), Würzburg, Germany E-mail: firstname.lastname@telematik-zentrum.de

^b Deutsches Zentrum für Luft- und Raumfahrt (DLR), Wessling, Germany E-mail: firstname.lastname@dlr.de

^c Max-Planck Institut für die Physik des Lichts, Erlangen, Germany E-mail: firstname.lastname@mpl.mpg.de

^d Friedrich-Alexander-Universität Erlangen-Nürnberg, Erlangen, Germany E-mail: firstname.lastname@fau.de

^e Ludwig-Maximilians-Universität, München, Germany E-mail: firstname.lastname@physik.uni-muenchen.de

^{*} Corresponding author

LEO	low	Earth	orbit

LEOP launch and early orbit phase

LMU Ludwig Maximilian University Munich

LVLH local-vertical-local-horizontal

MCU microcontroller unit

MPL Max Planck Institute for the Science of

Light

OBC on-board computer
OGS optical ground station

OGSOP optical ground station Oberpfaffenhofen
OSIRIS4QUBE optical space infrared downlink system

for QUBE

PAT pointing, acquisition and tracking

PCON payload controller QKD quantum key distribution

QRNG quantum random number generator

QSS quantum state sender
RF radio frequency
RFE receiver front end
RTC real-time clock

RTOS real-time operation system

RW reaction wheel

SWAPsize, weight, and powerTCPtransmission control protocolTIMtelematics international mission

TM telemetry

TOM telematics Earth observation mission

TTG time tagged guidance
UHF ultra high frequency
UTC coordinated universal time
ZfT Zentrum für Telematik

1. Introduction

As digital communication becomes increasingly vulnerable to advances in quantum computing, quantum key distribution (QKD) offers a method for exchanging encryption keys with information-theoretic security. Unlike classical cryptographic systems, QKD uses the principles of quantum mechanics to ensure that any eavesdropping attempt can be detected, making it a building-block for futureproof cybersecurity. However, terrestrial QKD networks are limited by fiber attenuation and line-of-sight constraints respectively, which restrict their scalability over long distances [1,2]. To overcome these limitations, satellite-based QKD has emerged as a promising solution for global quantum communication [3]. By transmitting quantum states through free-space links between satellites and ground stations, it becomes possible to establish secure keys across continents. In this context, CubeSats, which are miniature satellites built in standardized units, play a pivotal role. Their low cost, rapid development cycles, and increasing technological maturity make them ideal platforms for testing and deploying QKD technologies in orbit [4]. QUBE was designed as a technology demonstration mission to validate key components required for satellite-based QKD within a compact 3U CubeSat [5]. The goal was to reduce size, weight, and power (SWAP) of the QKD building blocks to scale the technology for future large-scale satellite networks [6, 7]. In order to meet the stringent demands of the CubeSat platform, photonic-integration technologies are employed to implement a quantum random number generator and optical quantum state sources.

This paper presents the results and lessons learned from the first year in orbit of QUBE. Section 2 outlines the satellite architecture and payload integration. Section 3 gives an overview of the satellite state after launch and early orbit phase (LEOP) and early commissioning. Section 4 details the ground segment and operational framework, including flight software with flexible on-board scripting and data handling. Section 5 focuses on the commissioning and performance of the attitude determination and control system (ADCS) as key component, which is essential for fine pointing during QKD experiments. Section 6 highlights the experimental procedures and results from in-orbit experiments, including the reliable establishment of the optical link between the optical ground station (OGS) and optical space infrared downlink system for QUBE (OSIRIS4QUBE). Section 7 gives an insight into the problems that occurred and the preliminary lessons learned. Finally, Section 8 discusses the next steps of the mission and future outlooks on technology demonstrations performed by CubeSats.

2. Mission Architecture

The goal of the QUBE mission is to demonstrate technologies that will enable QKD from a CubeSat as depicted in Fig. 1.

For this, the QUBE team came up with the mission architecture as shown in Fig. 2. The Ludwig Maximilian University Munich (LMU) and Max Planck Institute for the Science of Light (MPL)/Friedrich-Alexander-Universität Erlangen-Nürnberg (FAU) developed two experimental quantum state sender (QSS) generating strongly attenuated, coherent states, one with polarization encoding (at 850 nm QSS-8, LMU) and the other one demonstrating phase-space encoding (at 1550 nm QSS-C, MPL/FAU). Additionally, the MPL/FAU payload acts as payload controller (PCON). It controls the payloads and experiments and collects scientific data. Also, the MPL/FAU payload implements a quantum random number generator (QRNG)

IAC-25,B2,IPB,17,x9948 Page 2 of 16

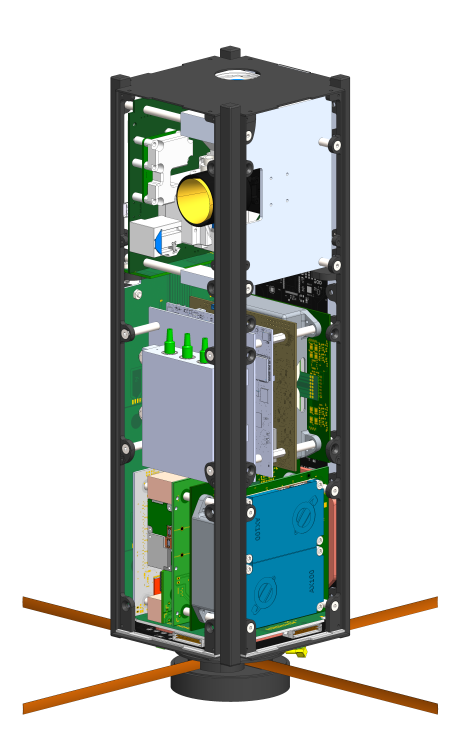


Fig. 1: CAD rendering of the QUBE CubeSat illustrating the integration of subsystems and payload components within the standardized 3U configuration.

to generate random sequences for the quantum states to be sent [6].

A highly miniaturized laser communication terminal (LCT) developed by German Aerospace Center (DLR) establishes the optical connection between the satellite and the ground station. OSIRIS4QUBE is the first evolution of OSIRIS4CubeSat [8], which extends the capabilities to operate with vastly different wavelengths (850 nm and 1550 nm), and to also accommodate the quantum payloads. In the QUBE mission, OSIRIS4QUBE transmits a clock signal over the classical optical link to allow the experimental payloads to synchronize with the single photon detection events at the ground station. Additionally, the classical signal is used by the OGS to actively track the satellite. To establish an optical connection between OSIRIS4QUBE and the OGS, an accurate pointing of the satellite of better than 1° is required [9].

The satellite bus built by Zentrum für Telematik (ZfT) consists of an on-board computer (OBC), an electrical power system (EPS), a communication subsystem (COMMS), an ADCS and five panels as depicted in Fig. 2. The ADCS integrates multiple sensors, including a star

tracker for precise attitude measurements, gyroscopes for angular velocity measurements, magnetometers for geomagnetic field measurements, and sun sensors for Sun vector estimation. These sensors provide the necessary data for real-time attitude determination. Actuation is achieved through a combination of miniature reaction wheels - two per axis - for fine torque generation, and five magnetorquers (one per panel), which interact with Earth's magnetic field to generate control torques. On the +z side, no magnetorquer could be placed since it is occupied by the laser aperture of OSIRIS4QUBE (see Fig. 1). The control architecture is distributed across several microcontroller units (MCUs), with each satellite panel hosting an MCU and an additional MCU per subsystem providing redundancy. The OBC is an MCU designed with full redundancy and minimal power usage. It functions as the primary controller for the UNISEC system bus. The lower backplane incorporates a backup array of deployment switches, whereas the longer backplane features an umbilical line connector and remove-before-flight switches. Both during and following satellite assembly, the umbilical line serves as a digital connection for troubleshooting, updating software in all subsystems, and performing battery upkeep. Interactions among subsystems and payloads are managed via the COMPASS protocol, which establishes a layered framework to convert each element into a universally reachable node, while delivering an extensive array of shared services to distribute capabilities across the entire satellite [4, 10].

3. LEOP and early Commissioning Phase

OUBE was launched on 16 August with the SpaceX Falcon-9 on the Transporter 11 mission. Following deployment, the OUBE satellite initiated its LEOP, during which core systems were activated and verified. Initial contact occurred during the first orbital pass over the Würzburg ultra high frequency (UHF) ground station, confirming deployed antennas and working EPS, OBC, and COMMS. The satellite successfully powered on after deployment and began autonomous detumbling, bringing its rotation rate within the targeted range of below 4 ° s⁻¹ during the first orbit, indicating healthy ADCS and panel components, i.e., the MCUs, magnetorquers, magnetometers, and gyroscopes. Subsystem commissioning proceeded with a structured verification of all sensor and actuator functionality, like performing attitude measurements with the star tracker, spin-up of all reaction wheels, taking Sun images with the Sun sensors, get global navigation satellite system (GNSS) fixes with all panels and monitoring of satellite state information like power consumptions and temperatures. During this, a magnetometer calibration was performed in orbit us-

IAC-25,B2,IPB,17,x9948 Page 3 of 16

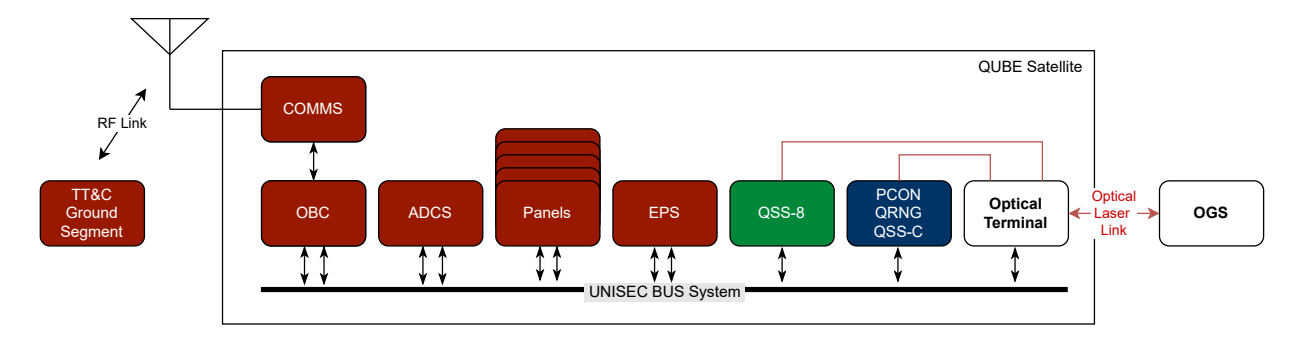


Fig. 2: The QUBE mission architecture, with the satellite bus related subsystems (red, ZfT), the PCON with QRNG, and quantum state sender QSS-C (blue, FAU/MPL), the OSIRIS4QUBE optical terminal (white, DLR) and the quantum state sender QSS-8 (green, LMU). The telemetry, tracking, and command via radio frequency (RF) is established using the ZfT ground segment located in Würzburg. The optical link is established with DLR's OGS in Oberpfaffenhofen.

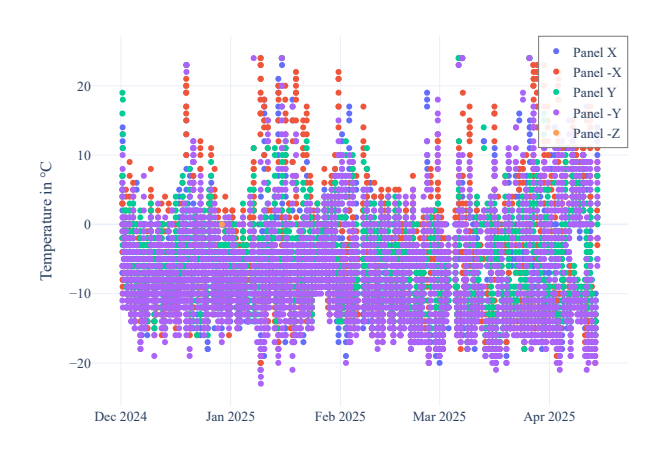


Fig. 3: Excerpt of the temperature monitoring on the panels of the satellite.

Table 1: Summary of subsystem status after LEOP.

Subsystem	Status After LEOP
COMMS	Antennas deployed, operational
EPS	Operational
ADCS	Calibrated, fine pointing verified
Panel +x	Calibrated
Panel -x	Calibrated, magnetometer
	anomaly
Panel +y	Calibrated
Panel -y	Calibrated
Panel -z	Calibrated
PCON / QSS-C	Health checks passed
QSS-8	Health checks passed
O4Q	Health checks passed

ing onboard scripting, achieving acceptable error margins despite internal magnetic disturbances (more in Section 5). The temperatures remained in the nominal range (compare Fig. 3) as well as the power consumption of all subsystems, indicating healthy state. A spin-up and detumbling test verified the capability of detumbling larger rotation rates before performing the first fine-pointing, to ensure safe behavior in case of some unexpected spin-up. The fine-pointing mode was validated in the first attempt on 26 September 2024, maintaining control errors below 0.5° throughout the overpass, with orthogonal axis deviations consistently under 0.2° [9].

Next, the payloads were commissioned to work step-bystep towards the first laser experiments. For this the PCON and OSIRIS4QUBE were commissioned, as well as their interaction with the ADCS mode management and operational procedures. The OSIRIS4QUBE terminal underwent a series of functional tests, including power consumption validation, beacon acquisition simulation, and closed-loop laser output verification. All results aligned with ground expectations, confirming readiness for optical tracking [9]. The quantum payloads QSS-8 and QSS-C could be initialized by the PCON, first characterization measurements of the QRNG have been performed [7], and communication with the other subsystems was verified. Power consumption indicated operation of the laser driver where signals from the lasers could not be validated, yet. A comprised summary of the satellite state after LEOP is given in Table 1.

IAC-25,B2,IPB,17,x9948 Page 4 of 16

4. Ground Segment, Flight Software and Operations

This section gives an overview of the operational environment, the satellite capabilities and the ground segment, serving as background for the experiment sections of the paper.

4.1 Optical Ground Segment

DLR uses the optical ground station Oberpfaffenhofen (OGSOP) for the reception of the laser signals [11]. The system is identical to the one used in the PIXL-1 mission [12]. The link establishment follows the pointing, acquisition and tracking (PAT) procedure. The OGS follows the satellite's path based on ephemeris files (consolidated prediction format (CPF)) provided by ZfT before the experiments. Two external laser beacons, mounted aside of the telescope's mount, generate an optical uplink signal to illuminate the satellite. OSIRIS4QUBE searches for and, if the satellite is pointing within the required accuracy of 1°, acquires the beacons. After the acquisition, OSIRIS4QUBE tracks the beacons actively with the same controller implementation as OSIRIS4CubeSat [8]. The OGS on the other hand, receives the transmission laser of the classical optical channel sent by OSIRIS4QUBE with an acquisition camera, operating in the infrared domain. This camera is externally mounted on the telescope and has an interface to the control of the telescope's mount. A closed loop tracking, based on the camera pictures mitigates offsets and enables the OGS accurate tracking of the laser. Fig. 4 depicts the operation of an optical downlink with the QUBE satellite.

The light received by the telescope itself is transferred through a coudé-path into a laboratory beneath the OGS. It gets reflected onto an optical table, which allows one to integrate multiple measurement setups in parallel. Mirrors and (dichroic) beam splitters steer and distribute the received signals to the various receivers or measurement devices. In the case of QUBE, a chromatic beam splitter separates the classical communication channel generated by OSIRIS4QUBE from the quantum channels, which in turn are guided to quantum state analysis set-ups for polarization and phase QKD-signals, respectively. The light of the classical channel is focused on a receiver front end (RFE) which does the optical-electrical conversion. The RFE receives the clock signal and forwards it electrically to the time taggers, to synchronize the received quantum states with the clock.

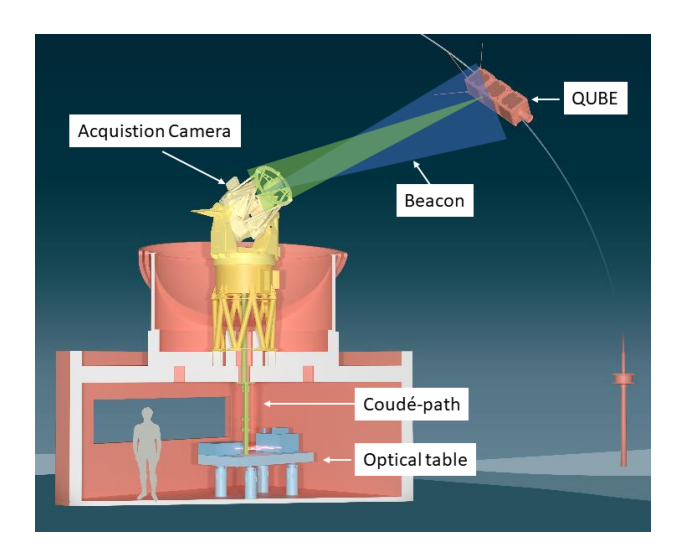


Fig. 4: Schematic view of the OGSOP during a QUBE downlink [11].

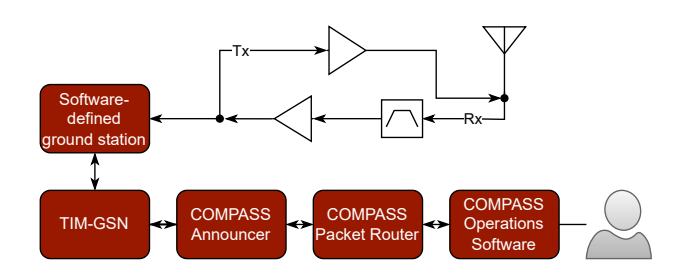


Fig. 5: The ground segment used for QUBE operations.

4.2 RF Ground Segment

As a ground segment for operating the satellite, the telematics international mission (TIM) ground station network (GSN) is used. The mission is integrated into the network as shown in Fig. 5. The satellite on-board protocol is COMPASS, which is accompanied by an operations software, providing the operator with a user interface to monitor the satellite state, issue commands, upload and download files, and perform other operational tasks [10]. For different mission phases, the operators can easily configure the view by adding/removing elements like a model-based subsystem settings view, monitoring panels, terminal-like command windows, graphs or the subsystem's file system (for file up- and download). An example of an operator view on a laser experiment is given in Fig. 6, illustrating a subset of the mentioned user interface elements. Multiple instances of this software can connect via transmission control protocol (TCP) to a COMPASS packet router. This router allows for example to filter COM-PASS packets, provides packet recording, has additional

IAC-25,B2,IPB,17,x9948 Page 5 of 16

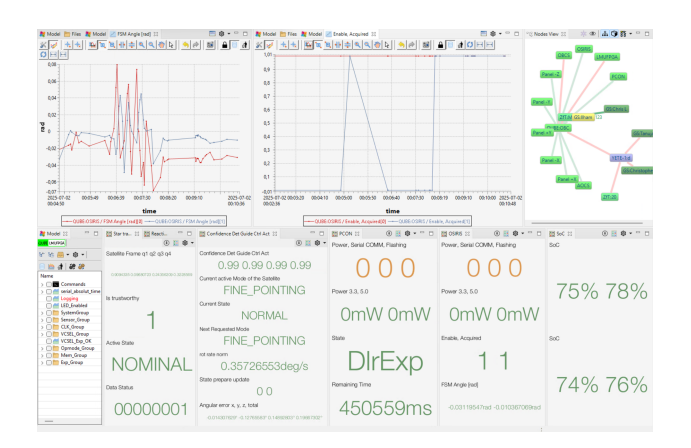


Fig. 6: The COMPASS operations software used for QUBE operations. This example shows an operator's perspective on monitoring a laser experiment.

monitoring and evaluation features, and is responsible for security aspects like replay protection. This router is connected to the QUBE COMPASS Announcer, which is an adapter from COMPASS to the radio protocols and also implements the interface to the TIM-GSN, i.e., providing orbit information, frequency, modulation, etc. Through TIM-GSN, the radio packets are provided to an available ground station, which schedules the overpasses, computes Doppler information and tracking state (i.e., azimuth and elevation angles) and eventually transmits the packets. In QUBE, primarily the UHF stations in Würzburg operated by ZfT are used. An evaluation of the down-linked data in the first year of QUBE is shown in Fig. 7. The different APIs indicate different operational phases. During the first weeks, reception issues due to local radio frequency (RF) interference reduced traffic, limiting the satellite operation to smaller telecommands and telemetry requests via the command (CMD) and the generic data system (GDS) API. Data generated on the satellite bus subsystems is downloaded with the file API, whereas the payload subsystems use the downlink API for this. Weeks with lower data were typically upload-heavy (e.g., software update upload). In total, around $56\,\mathrm{MB}$ of data have been collected during the first year.

4.3 Flight Software

This section details the key components of QUBE's flight software, which is structured around two distinct architectural approaches to meet the mission's diverse operational needs.

The OBC software is designed to manage the most critical functions for the satellite's survival and communication.

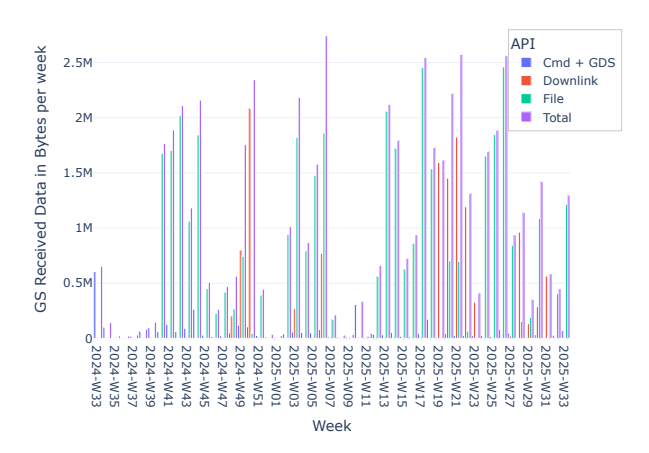


Fig. 7: The amount of data downloaded from QUBE on the respective COMPASS APIs over the first year.

Its primary focus is reliability through simplicity, achieved by employing a traditional big loop architecture suitable for non-time-critical tasks like power management and software updates.

Conversely, the software for the ADCS and panels is built around a real-time operation system (RTOS). Here, timing is the most critical aspect, as these components must perform rapid sensor sampling and execute closed-loop control in real-time to achieve the high pointing accuracy required for mission success.

The following sub-sections will provide a detailed overview of the key features of both the OBC software and the RTOS-based software.

4.3.1 OBC

The OBC serves as control central unit of the satellite, managing its most critical operations. It performs several key functions to ensure the satellite runs smoothly and can adapt to changing conditions.

A primary function of the OBC is to manage the satellite's power. It continuously monitors the EPS and, based on the battery's state of charge, enters different power modes. This allows it to strategically power on and off various subsystems, ensuring the satellite's power consumption never exceeds what the solar panels can generate. This control is critical for preventing a complete power drain and keeping the satellite operational.

Another key feature is the ability to perform firmware updates of the subsystems. By uploading a new firmware binary to the OBC, each subsystem can be updated in space, including the OBC itself. This capability is vital for fixing

IAC-25,B2,IPB,17,x9948 Page 6 of 16

software bugs, patching security vulnerabilities, and introducing new features throughout the mission's lifetime.

The OBC acts as the central communication gateway for the satellite's radios. Immediately after the satellite is deployed from its launcher, the OBC is responsible for initiating radio antenna deployment. All data packets between the ground station and the OBC pass through the OBC, which manages and regulates packet flow to make efficient use of the available communication link. Monitoring the time since the last received ground packet allows for the detection of communication failures. If a certain amount of time passes without a signal, the OBC can trigger recovery actions, such as switching to a backup radio or performing a complete satellite power cycle after four days.

Finally, the OBC serves as the time synchronization manager for the entire satellite. Each subsystem manages its own time data from every available time source, including the internal real-time clock (RTC), timestamps from ground packets, and data from the GNSS receiver, if available. The subsystems's time accuracy is provided to the OBC, which in turn selects the most accurate one as satellite-synchronizer. The satellite synchronizer broadcasts a future coordinated universal time (UTC) timestamp that specifies when it will drive the dedicated electrical synchronization line high. Each subsystem stores this value in advance. When the rising edge of the sync line occurs, every subsystem sets its internal UTC time to the stored timestamp, achieving simultaneous synchronization. This process is highly precise, achieving a standard deviation of just 52 µs across all subsystems. With this accuracy, contribution to the resulting pointing error budget in the QUBE mission can be neglected.

4.3.2 Panels & ADCS

To meet the stringent timing and responsiveness requirements of both the sensor and control loops, FreeRTOS is used on all panels and within the ADCS [13]. It ensures deterministic, predictable task scheduling and robust task prioritization. The overhead of task-switching is minimal, so the limited onboard resources, such as CPU, memory, or power, are used efficiently.

To further strengthen the robustness of the system, a watchdog that oversees all the tasks of the RTOS is implemented. Each task has a predefined period during which it has to notify the watchdog. In case a task does not report back in time repeatedly, e.g., due to faulty behavior, the watchdog resets the system. On reset, full information of the system state, such as the program counter or the active thread, is gathered. This information is available to the

operators after a reboot to identify the root cause of the reset.

The panels and the ADCS also feature extensive logging and recording support. While its main purpose is to record experimental data onboard the spacecraft, it can be used for debugging and detection of faulty behavior as well. Logging is used primarily for writing single-occurrence time-stamped events to a file in human-readable string format. Five different severity levels are supported and can be activated incrementally as needed, which allows for efficient usage of available memory and bandwidth.

Contrary to logging, the recording feature focuses on capturing (repeating) real-time data, including sensor data, filter states, or health information. All the data is stored efficiently in a binary format, which has to be decoded on the ground. Recordings are started via telecommand, which also allows for adjusting the sample rate or timestamp format. Both logging and recording operate fully asynchronously, so high-priority tasks are not affected even by extensive recording during experiments.

Instead of typical time-tagged commands, a scripting environment is implemented on the satellite. The scripting environment builds on top of the Jerryscript engine so the chosen programming language for scripting is JavaScript [14]. Scripts have full access to all the commands and settings a human operator has. Multiple ways to start a script are available, including operator commanding, automatic start on boot-up, or time-tagged execution based either on uptime or UTC. This effectively covers all the functionality of traditional time-tagged commands. The strength of scripts is that they can also observe the state of the satellite. With this, scripts can also take actions based on the satellite's state without operator interaction, significantly boosting the degree of automation available to satellite operations. With this, whole features - like a new controller - can be easily added [12]. Additionally, this is especially important for the reliable preparation of the experiments, where there is only limited or no contact with the ground.

5. Attitude Determination and Control System

In this section, we present the ADCS, which is of high relevance in performing the planned experiments in this mission. We showcase some commissioning and validation steps before performing the first laser experiments.

5.1 Overview

The core components of the QUBE ADCS include magnetorquers and reaction wheels (RWs) for actuation, along

IAC-25,B2,IPB,17,x9948 Page 7 of 16

with Sun sensors, magnetometers, gyroscopes, and a star tracker for attitude determination. Upon deployment, the satellite enters the detumbling mode, where the angular rates are reduced with magnetorquers to acceptable limits. This initial stabilization is essential for enabling subsequent attitude control operations. In the event of system anomalies or critical failures, the safety mode is activated. This configuration minimizes subsystem activity for failure avoidance, e.g., prevents satellite spin-up due to sensor anomalies. To optimize energy acquisition, the Sunpointing mode aligns the satellite solar panels toward the Sun, maximizing power generation while protecting sensitive optical components. For initial payload alignment, the coarse-pointing mode is employed, relying on Sun sensor, magnetometer and gyroscope information and using RWs as actuators. This prepares the fine-pointing mode, which requires the course alignment for getting a star tracker fix. This mode is implemented to achieve sub-degree pointing accuracy required for the optical laser link [15]. When the optical link is established, the ADCS can switch to relative control based on the fine steering mirror (FSM) angle measurement provided by OSIRIS4QUBE for the remaining overpass, which is independent of star tracker and gyro measurements [16]. Achieving the sub-degree pointing accuracy to establish the optical link reliably was the major challenge for the ADCS. Due to this, extensive ground tests based on turntable-based [17] and air-bearingbased [18] testbeds were performed prior to launch. During this, several issues, e.g., with the selected star tracker were observed and mitigated [16, 17].

5.2 Commissioning Tests and Results

Several in-orbit commissioning tests were conducted to validate the functionality of the ADCS. These comprised sensor-health assessments, magnetometer calibration, gyroscope verification, magnetorquer polarity checks, and detumbling experiments, among others. The sequence followed a logical order, starting with sensor evaluations, followed by actuator tests, and concluding with verification of the ADCS operational modes. Selected tests of particular interest and their results are presented below.

5.2.1 Magnetometer Tests and Calibration

One of the initial in-orbit tests focused on validating the on-board magnetometer sensors. Each panel-mounted magnetometer was calibrated for bias, scale, and misalignment. The procedure involved collecting raw measurements from all panels and comparing their magnitudes against the international geomagnetic reference field

Table 2: Summary of the ADCS operational modes for QUBE.

Mode	Description
Detumbling	Stabilizes the satellite after deploy-
	ment using magnetorquers to reduce
G . C .	angular rates to safe levels.
Safety	Minimal activity mode used in case
	of critical system failure; prioritizes
	system integrity and power conser-
	vation.
Sun-pointing	Aligns solar panels toward the Sun
	to optimize power generation and
	protect sensitive optical compo-
	nents.
Coarse-pointing	Orients the satellite toward the
	ground station using onboard sen-
	sors and precomputed tracking data.
Fine-pointing	Achieves high-precision alignment
Tine-pointing	0 1
	using star tracker data, gyroscope
	fusion, and real-time optical bea-
	con tracking after link establish-
	ment [16].

(IGRF) data. The objective was to minimize both the absolute error relative to the reference field and the relative error among the sensors. After calibration, the measurements along each individual axis showed a consistent alignment across all subsystems, as illustrated in figures 8, 9 and 10.

5.2.2 Magnetorquer and Detumbling Verification

To verify the magnetorquer polarity in orbit, the five panel-mounted magnetorquers (+x, -x, +y, -y, and -z) were sequentially actuated at maximum dipole strength in both polarities for a fixed duration. The main objective was to confirm that the soldering and electrical connections had withstand the launch loads. Each magnetorquer integrates a dedicated coil magnetometer within its enclosed area, which records the induced magnetic field and enables indirect measurement of the dipole moment. These sensors are independent of those used in the ADCS control loop and are used solely for magnetorquer verification. All measurements are reported in the local magnetometer frame, with the z-axis aligned to the magnetorquer axis. As expected, polarity switching produced a corresponding inversion of the measured z-axis field in the corresponding magnetometer, as shown in Fig. 11.

IAC-25,B2,IPB,17,x9948 Page 8 of 16

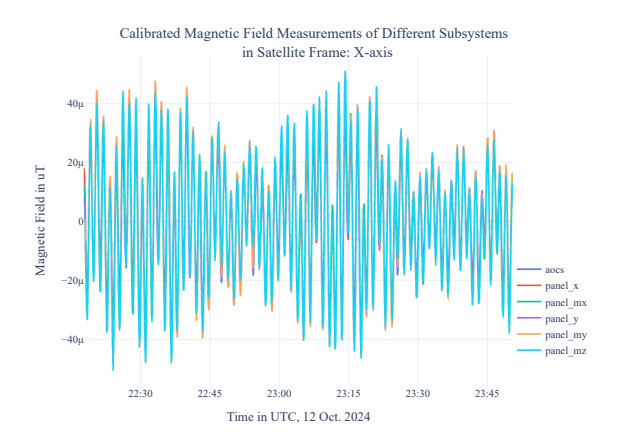


Fig. 8: Validation of Magnetometer in orbit calibration about x-axis.

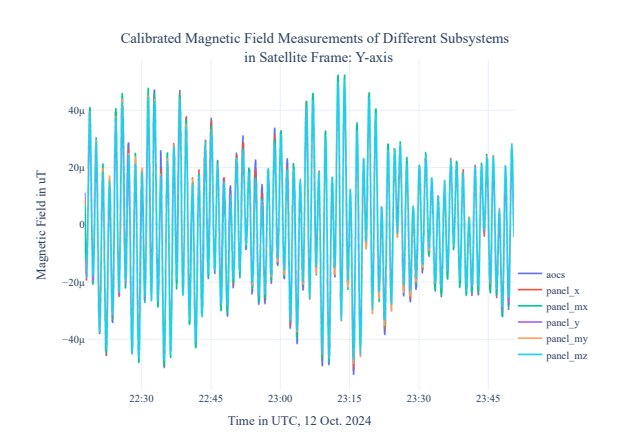


Fig. 9: Validation of Magnetometer in orbit calibration about y-axis.

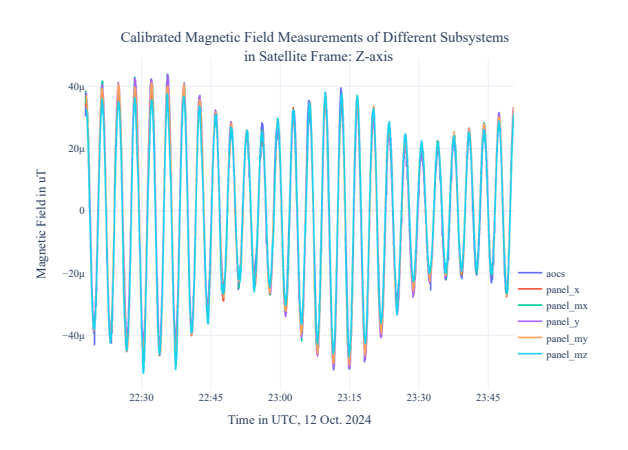


Fig. 10: Validation of Magnetometer in orbit calibration about z-axis.

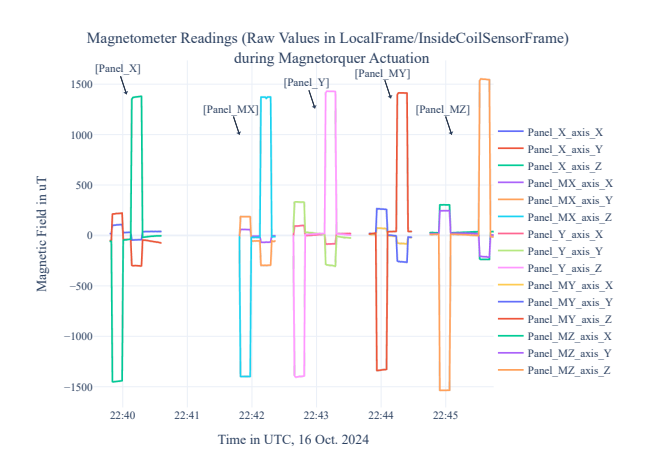


Fig. 11: Magnetometer measurements during magnetorquer actuation on all five panels.

During QUBE's first orbit, the detumbling controller reduced the satellite's rotation rate to between $2.5\,^{\circ}\,\mathrm{s}^{-1}$ and $4\,^{\circ}\,\mathrm{s}^{-1}$ [9]. To evaluate the controller's performance at higher initial rotation rates, as well as to verify the activation logic and rotation-rate threshold parameters, a dedicated detumbling test was conducted. Analyses of typical CubeSat post-deployment rotation rates indicate that an initial rate of approximately $10\,^{\circ}\,\mathrm{s}^{-1}$ is representative, so this value was chosen as the starting point for the test.

Fig. 12 shows the rotation rates during the detumbling test. In the first phase, starting at 22:53, a spin-up controller (implemented as a script) was activated to increase the rotation rate from $1 \circ s^{-1}$ to approximately $10 \circ s^{-1}$ within about 20 minutes. In the second phase, the spin-up controller remained active to ensure that the rotation rate stayed above 10 ° s⁻¹. Shortly after 01:00, sudden temporary decrease in the rotation rate occurred, likely due to erroneous data from one of the gyroscopes. The anomaly was detected, and the system successfully switched to another gyroscope, restoring correct measurements. At 02:08, the third phase began: The detumbling controller was enabled, reducing the satellite's rotation rate from $10^{\circ} \,\mathrm{s}^{-1}$ to $2.5 \,^{\circ}\,\mathrm{s}^{-1}$ within one hour, and subsequently to about $1.5 \,^{\circ} \, \mathrm{s}^{-1}$. This test demonstrated not only the functionality and robustness of OUBE's detumbling controller, but also the capability of the scripting framework to implement efficient attitude control algorithms.

5.2.3 GNSS Receiver and Orbit Determination

A prerequisite for the precise pointing of the satellite and the OGS is a precise knowledge of the satellite's orbit.

IAC-25,B2,IPB,17,x9948 Page 9 of 16

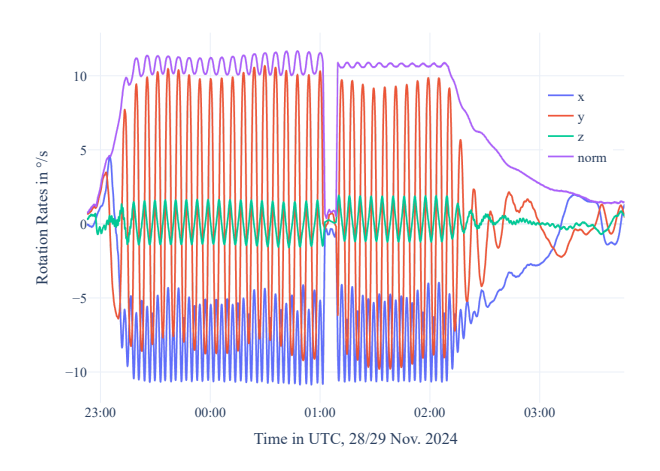


Fig. 12: Rotation rates during the spin-up and detumbling test.

QUBE is equipped with four GNSS receivers, one on each of its four long panels. During commissioning, it became evident that the quality of the GNSS data was significantly lower than anticipated based on on-ground GNSS simulator results.

Three of the four receivers had difficulties in acquiring a reliable fix and provided valid navigation solutions only intermittently and predominantly in the southern hemisphere. Furthermore, several major outliers, ranging from 200 to 1000 km and lasting for several minutes, were observed with no apparent correlation to known regions of poor GNSS quality, such as those caused by jamming or spoofing.

Velocity estimates exhibited a consistent bias in the radial direction across all panels and were, therefore, completely excluded from the orbit determination process. Exemplary post-fit residuals for the position and velocity in the local-vertical-local-horizontal (LVLH) frame are presented in Fig. 13. While the position fit was significantly better than the velocity fit, the radial component of the position also displayed a slight bias, and its accuracy fluctuated throughout the orbit. This behavior was not observed during on-ground GNSS simulator tests before launch, where the one-sigma position error was approximately 8 m.

A significant challenge encountered during commissioning was the accuracy of orbit prediction. This was exacerbated by the solar maximum of the 25th solar cycle, which was reached in October 2024. This period of high solar activity resulted in considerable uncertainty in atmospheric density. Given that atmospheric drag is the dominant factor influencing prediction error for low Earth orbit (LEO) satellites, this directly impacted the mission's

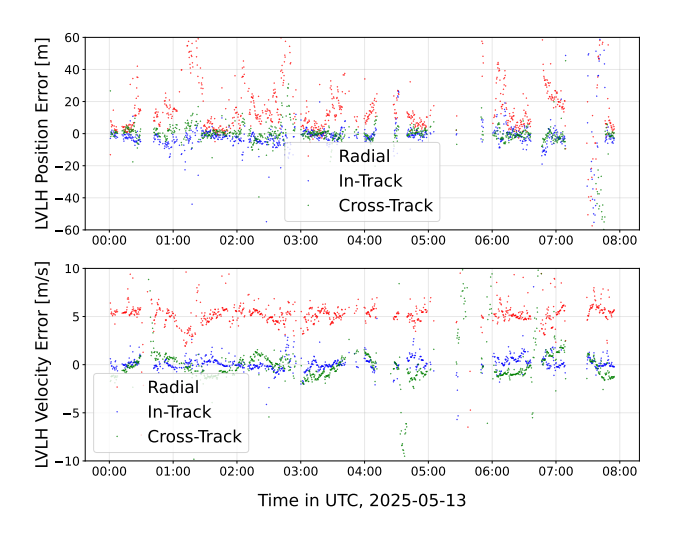


Fig. 13: Orbit determination residuals in LVLH frame for 13 May 2025 time tagged guidance (TTG) recording

ability to meet the stringent orbit prediction accuracy requirement of a $150\,\mathrm{m}$ uncertainty for the OGS.

This challenge necessitated a procedural change: recording GNSS data on the day preceding experiments to generate the CPF files as close to the experiment as possible. The implementation of this new procedure (cf. Fig. 15), combined with improvements in the orbit determination process - such as the integration of more advanced outlier filters and more frequent updates of space weather data - successfully enabled the mission to meet its orbit determination requirements.

A typical prediction for a CPF file during an experiment is shown in Fig. 14. While the +x panel was the primary choice for most experiments due to its superior navigation data, further analysis confirmed that mission success could also be achieved with less accurate GNSS receivers. With this, despite these numerous challenges, the commissioning of all the GNSS receivers and the orbit determination system was successfully completed.

6. Scientific Experiment Preparation and Execution

The procedure for the laser experiment was carefully established with the following considerations in mind:

- Precise timing: ensuring that all steps are executed at strict and well-defined time intervals to meet experiment requirements.
- Single ground station usage: plan with the use of the UHF ground station in Würzburg only.

IAC-25,B2,IPB,17,x9948 Page 10 of 16

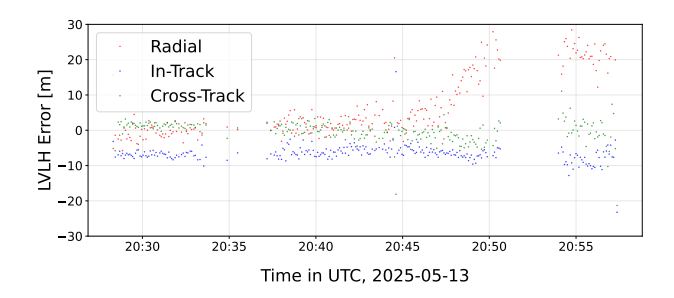


Fig. 14: CPF orbit prediction error in LVLH frame for experiment on 13 May 2025

- Payload protection: safeguarding the optical payload throughout all operational phases to prevent damage or degradation.
- Operational efficiency: minimizing the preparation time required on-ground prior to an experiment, while ensuring high reliability during execution.
- Failure handling: preparing for contingencies, such as rare subsystem resets triggered by watchdogs, by including recovery strategies within the procedure.
- Experiment continuity: enabling the performance of laser experiments over consecutive satellite overpass.
- Automation: leveraging auto-start folder and scheduling to reduce human error and mitigate missed execution windows.

6.1 Experimental Procedure

To address the operational requirements, the scripting capability onboard the panels and ADCS was utilized. It enables automated time-tagged command execution and satellite state monitoring, thereby reducing the operator's workload to file upload and download. The timeline of the laser experiment is shown in Fig. 15. Experiment planning is jointly carried out by the satellite and OGS operators, with overpass selection depending on maximum elevation and local weather conditions at the OGS location. The satellite operators then prepare scripts containing the experiment-specific timings as well as GDS settings. Each script is first validated through a test on the engineering model (EM) before being uplinked to the satellite file system.

Prior to the start of the experiment, the rotation rates of the satellite are reduced below $2^{\circ} \, s^{-1}$ for GNSS acquisition. The downloaded GNSS data is post-processed on ground to generate the time tagged guidance (TTG) file

required for accurate satellite pointing during the experiment. Commissioning tests showed that orbit prediction accuracy is highest when GNSS data is recorded as close as possible to the experiment. Therefore, this process is repeated at least 5 h prior to the experiment to compute the CPF file for OGS tracking. In cases where no GNSS data download was possible prior to the experiment, the data used for the TTG file is also used to generate the CPF, thus providing redundancy. This approach proved to be reliable for conducting the experiment. To further reduce risk, all scripts are marked to be executed directly after the systems boots to ensure automatic initiation, with the only residual failure mode being a file system issue preventing script execution.

During this preparation phase, the ADCS parameters for fine pointing - such as controller gain and star tracker settings - are configured. At the start of the experiment, the satellite automatically transitions into fine pointing mode. The payloads are activated via script once the satellite rises above 5° elevation at the OGS. The actuation of the OSIRIS4QUBE via PCON provides an additional safeguard against accidental laser activation.

During the experiment, payload and ADCS telemetry (TM) are continuously transmitted over the UHF link, allowing real-time monitoring from Würzburg. After completion, the TM recordings from the ADCS and panels, together with the payload log file on PCON, are downlinked during subsequent passes. This data is essential for analyzing performance and optimizing future experiments.

6.2 Experiments and Results

The first experiment was conducted on 2 May 2025, during which the beacon signal was tracked for approximately four minutes, with interruptions cause by clouds and a short restart of the OGS tracking system. The beacon signal transmitted from QUBE was recorded by an infrared camera installed at the optical table of the OGS, as shown in Fig. 16. After that, seven additional laser experiments were performed, of which only one failed to establish the tracking of the laser. In this case, telemetry indicated nominal system behavior, leaving the cause of the missing signal acquisition uncertain. Possible explanations include low elevation combined with thin cloud cover, or an increased rotation rate around the z-axis to avoid star tracker blinding. An overview of all experiments is given in Table 3. All successful trackings lasted significantly longer than those achieved in previous missions with DLR's optical terminal (1:48 min [12]), highlighting the reliability of the ADCS and the benefits of extensive on-ground test-

IAC-25,B2,IPB,17,x9948 Page 11 of 16

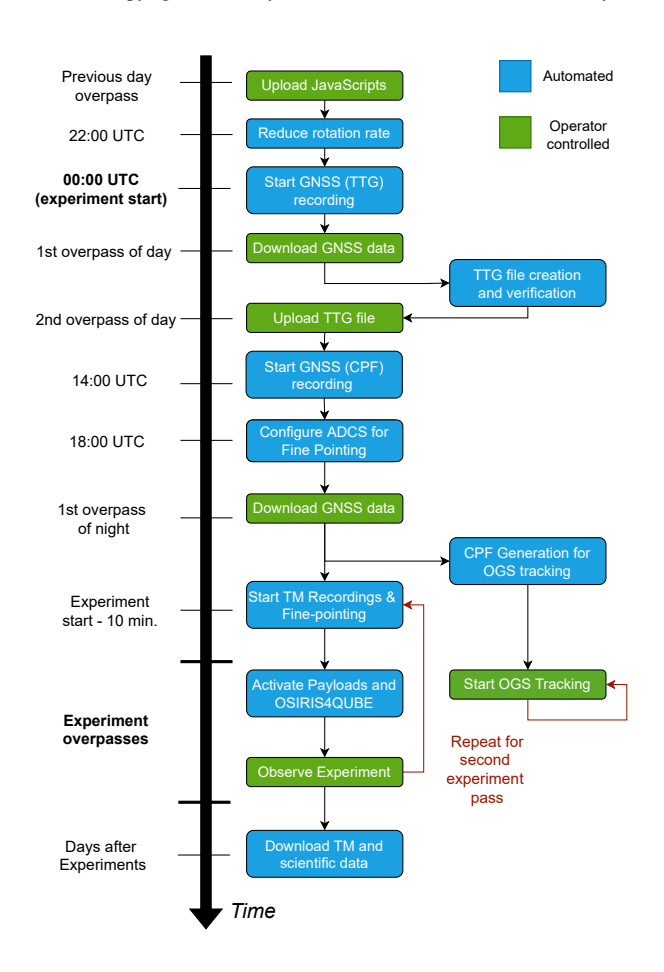


Fig. 15: Procedure description of a laser experiment including preparation steps.

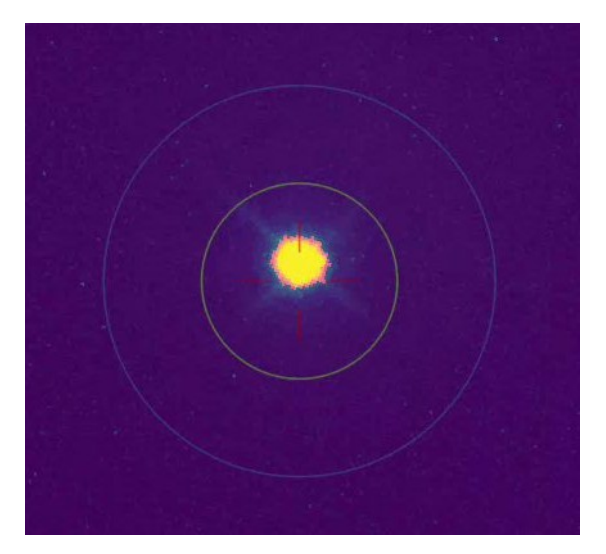


Fig. 16: The laser spot emitted from QUBE by OSIRIS4QUBE as seen at the OGS on its optical table.

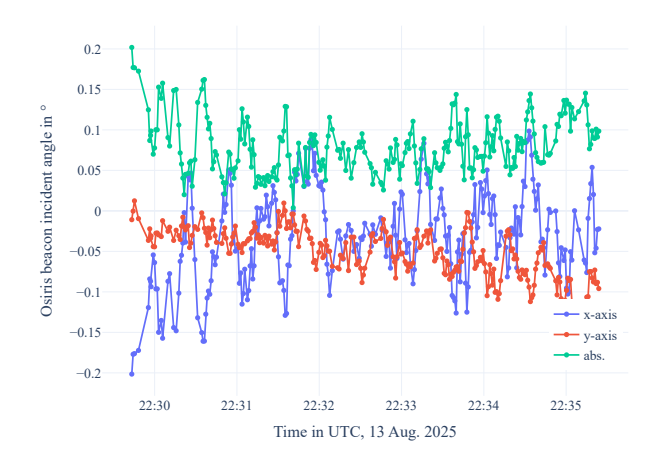


Fig. 17: The OSIRIS FSM angle offsets during the experiment EX07, giving as 3σ standard deviation of 0.10° , including ADCS pointing error, FSM pointing error and atmospheric signal fluctuations.

ing. The measured incident angles at OSIRIS4QUBE, shown in Fig. 17, provide further evidence of the pointing performance. In this experiment, the 3σ standard deviation was 0.10° , demonstrating stable pointing within the requirements. Mean offsets of -0.03° in x and -0.05° in y indicate a significant improvement with regards to the ADCS-OSIRIS4QUBE integration compared with the previous PIXL-1 mission [8].

From the perspective of OSIRIS4QUBE, the first downlink attempts were successful. The ground station beacon was reliably detected, validating the design of the search pattern. During tracking, the tracking error remained within the transmitted beam divergence, as measured by the internal four-quadrant diode. This allowed verification of the design adjustments and performance measurements conducted on the integrated satellite [19]. Low-frequency fluctuations in intensity were detected with the OGS. To exclude a potential misalignment between the transmit and receive path in OSIRIS4QUBE, intensity peaks were compared with the satellite attitude and pointing direction, revealing no correlation (see Fig. 18).

Due to automation, it is technically feasible to use every night overpass for performing laser experiments (as demonstrated with the experiments E06, E07 and E08, compare Table 3). For this, the preparation steps required on the day before the experiment are executed together with the preparation steps of the running experiment. However, it is not possible to download the telemetry on-board the satellite in this case, since the following overpasses are already required for preparation of the next experiment.

IAC-25,B2,IPB,17,x9948 Page 12 of 16

Table 3: Overview of QUBE laser experiments, covering max. elevation angle $\epsilon_{\rm max}$ of the pass and the duration of tracked laser signal. This table covers all experiments without errors in operational procedure, i.e., satellite was in correct mode, the weather allowed to operate the OGS, and OSIRIS4QUBE was active.

ID	Date	$\epsilon_{ m max}$	Track.	Comment
E01	25-05-02	68°	4 min.	Partial Clouds,
				OGS restart
E02	25-05-13	48°	7 min.	Signal tracked
				during almost the
				whole pass
E03	25-07-01	28°	5 min.	CLK signals re-
				ceived
E04	25-07-22	65°	5 min.	
E05	25-08-07	14°	0 min.	No tracking acq.,
				low ϵ_{\max}
E06	25-08-12	40°	5 min.	FSM offset varied
				leading to drop
				outs
E07	25-08-13	20°	6 min.	Tracking over
				whole overpass
				without drop-out
E08	25-08-13	32°	3 min.	Consecutive pass
				after E07

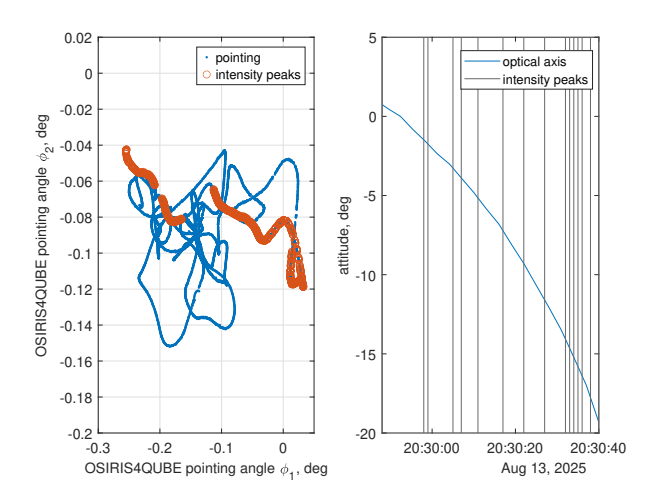


Fig. 18: Pointing orientation to observed intensity peak at the OGS yielded no significant correlation.

Regarding the quantum payloads, first successful experiments were conducted, where it was demonstrated that functional blocks of the optical part of the QRNG work as expected [7].

7. Challenges and Preliminary Lessons Learned

Several operational challenges emerged during QUBE's first year in orbit. While some of these challenges have been mentioned throughout the paper, this section provides an overview in Table 4, summarizing each issue along with its corresponding mitigation strategy, and highlights additional lessons learned from the first year of operations. During some parts of the first downlinks, DLR observed power fluctuations of the optical signal received by the OGS. Although the signal was received uninterruptedly, the signal strength varied more than expected and experienced in previous projects. The fluctuations were observed only by the infrared camera. So far no optical power meter was integrated on the optical table to evaluate the fluctuations in detail. Neither the satellite telemetry nor the controller values of OSIRIS4QUBE showed correlations to these fluctuations. Furthermore, it can be said that they appear at a relatively low frequency so that atmospheric effects can be ruled out. The next step is to characterize these fluctuations with an optical power meter, analyze if the received optical power is still sufficient and to investigate into stabilizing the connection during these phases.

A recurring 'Guidance File Error' was traced to residual trajectory data in memory from the previous experiment, which prevented mode transition to fine pointing. This was resolved via a software patch and an interim reset procedure.

Time synchronization between the panels and the OSIRIS4QUBE laser terminal was initially blocked by bus separation and a related configuration mistake; a custom data relay implemented in onboard scripts restored synchronization.

Additionally, packet loss during downlink disrupted file transfers from PCON, requiring adaptations to ground-side processing [9].

Another aspect is the limited amount of data which can be downloaded via the small bandwidth of the UHF link. A typical laser experiment generates around 3 MB of telemetry data, which requires around 1 week to download with a single UHF ground station. To mitigate this issue, additional ground stations would be needed, or the data rate would have to be increased by the use of a higher bandwidth, e.g., with an S-band transceiver as planned in the follow-on mission QUBE-II [20].

In addition, a problem with temperature-dependent

IAC-25,B2,IPB,17,x9948 Page 13 of 16

Table 4: Key challenges and mitigation strategies observed in the first year of operation.

Challenge	Mitigation Strategy
UHF Signal Interference	Filter with a smaller pass-band on ground side.
Repeated fine pointing	Subsystem reset for temporary mitigation -> final fix with software update.
Unreliable GNSS Data	Scheduled sampling with a script to gather more data.
OSIRIS4QUBE time synchronization	Script implementing a time broadcast relay to OSIRIS4QUBE.
Initial magnetometer on-ground calibration not matching in-orbit	Performed in-orbit calibration.
Anomaly with magnetometer on panel +x	Rely on the other panel measurements.
OSIRIS4QUBE mirror angles time information missing	Script adding timestamp automatically with checks.
Complex operation procedure with high operator effort leading to errors and high personal effort	Automated most steps with scripting.
PCON Bus issues	Temporary stop of use, on-ground reproduction and software update.
PCON file downlink issues due to wrong chunk order and	Adaptation on ground software to reorder chunks and throt-
timing	tle chunk requests, added inter-subsystem file transfer to
	ADCS and download from there.
OSIRIS4QUBE power fluctuation	Detailed analysis to exclude satellite bus correlation.
RW config fallback	Script turning on RWs periodically for 5 minutes to run health procedures.
QRNG entropy estimation problems	Software update with improved algorithms.

gyro calibration was observed and fixed after launch, which will be mitigated in advance in future missions like CloudCT [21] with an improved on-ground calibration procedure.

Also, in preparation to generate quantum random numbers, MPL/FAU encountered problems with the automated calibration and entropy estimation routines of the QRNG, which however are tackled by improved algorithms. For this, the software was updated.

Even though the QKD payloads could be turned on and the power consumption when operating the laser diodes seems to be nominal, rigorous onboard testing of the entire QKD system was not possible due to hardware limitations. The full functionality can only be verified with an actual QSS downlink. This will be improved for future missions with more onboard testing capabilities.

8. Conclusion and Outlook

The successful and reliable establishment of optical links demonstrated both the high-precision pointing capabilities of the ADCS and the operational maturity of OSIRIS4QUBE. For OSIRIS4QUBE, it verified the development transition from a classical LCT towards QKD

capabilities on CubeSats. With multiple successful downlinks, it could be shown that the lessons learned and insights from DLR's PIXL-1 mission, which were taken into account in the design of the QUBE mission, were highly beneficial. The QKD capabilities of OSIRIS4QUBE will be verified in the upcoming experiments, when including the partner payloads into the operation.

Notably, the ratio of successful links with ZfT's satellite bus could be increased significantly. In addition to improved mechanical integration, a primary reason lies in the on-ground validation of the ADCS, which allowed potential issues (such as those encountered with the star tracker during the PIXL-1 mission) to be identified and mitigated prior to launch [15, 17]. For instance, also an additional beacon-enhanced tracking mode was developed to reduce star tracker dependency and to use the precise FSM measurements of OSIRIS4QUBE on the ADCS [16]. The next step is the demonstration of the QRNG and to generate and receive optical signals from the quantum payloads. These generated signals are of high relevance for QKDprotocols to obtain secure keys. With the experience gained in QUBE, the follow-up mission QUBE-II is already on the horizon [20]. QUBE-II is planned for launch mid of 2026. The modular approach of OSIRIS4QUBE allows to extend

IAC-25,B2,IPB,17,x9948 Page 14 of 16

its capabilities to fulfill the requirements of the LCT for the QUBE-II project. Therefore, OSIRIS4QUBE can be used as a system architecture base to reduce development time, costs, and risks. The operational experiences gained in this challenging CubeSat mission will be transferred to further missions like the telematics Earth observation mission (TOM) [22] and CloudCT [21]. This includes the reuse and automation of LEOP and commissioning with the JavaScript scripts. In addition, the main subsystems, including components like the EPS, COMMS, OBC, panels and parts of the ADCS will be reused to ensure fast and reliable satellite development and deployment.

Acknowledgements

This research was carried out within the scope of the projects QUBE and QUBE II, funded by the German Federal Ministry of Research, Technology and Space (BMFTR).

References

- [1] Stefano Pirandola, Ulrik L Andersen, Leonardo Banchi, Mario Berta, Darius Bunandar, Roger Colbeck, et al. Advances in quantum cryptography. *Advances in optics and photonics*, 12(4):1012–1236, 2020.
- [2] Feihu Xu, Xiongfeng Ma, Qiang Zhang, Hoi-Kwong Lo, and Jian-Wei Pan. Secure quantum key distribution with realistic devices. *Rev. Mod. Phys.*, 92:025002, May 2020.
- [3] Chao-Yang Lu, Yuan Cao, Cheng-Zhi Peng, and Jian-Wei Pan. Micius quantum experiments in space. *Reviews of Modern Physics*, 94(3):035001, 2022.
- [4] Ilham Mammadov, Julian Scharnagl, Roland Haber, and Klaus Schilling. Quantum key distribution for secure communication by nano-satellites. In *Proceedings of the 73rd International Astronautical Congress (IAC)*, 2022.
- [5] Lukas Knips, Michael Auer, Adomas Baliuka, Ömer Bayraktar, Peter Freiwang, Matthias Grünefeld, et al. QUBE–towards quantum key distribution with small satellites. In *Quantum 2.0*, pages QTh3A–6. Optica Publishing Group, 2022.
- [6] Jonas Pudelko, Ömer Bayraktar, Imran Khan, Winfried Boxleitner, Stefan Petscharnig, Christoph Pacher, et al. Integrated photonics for quantum communication on a cubesat. In *Proceedings of Conference on Lasers and Electro-Optics/Europe*

- (CLEO/Europe 2023) and European Quantum Electronics Conference (EQEC 2023), page eb_6_4. Optica Publishing Group, 2023.
- [7] Jonas Pudelko, Ömer Bayraktar, Joost Vermeer, Luca Vill, Imran Khan, Winfried Boxleitner, et al. Quantum Communication with Photonic Integrated Circuits on a CubeSat. In 2025 Conference on Lasers and Electro-Optics Europe & European Quantum Electronics Conference (CLEO/Europe-EQEC), pages 1– 1, June 2025.
- [8] René Rüddenklau, Fabian Rein, Christian Roubal, Benjamin Rödiger, and Christopher Schmidt. Inorbit demonstration of acquisition and tracking on OSIRIS4CubeSat. Optics express, 32(23):41188– 41200, 2024.
- [9] Benjamin Rödiger, René Rüddenklau, Lisa Elsner, Timon Petermann, and Philip Bangert. First in-orbit results of the qube mission hosting a laser communication terminal for experiments towards quantum key distribution from cubesats. In *Proceedings of* SmallSat Europe 2025, 05 2025.
- [10] Veaceslav Dombrovski. *Software framework to support operations of nanosatellite formations.* PhD thesis, Universität Würzburg, 2022.
- [11] Johannes Prell, Alexander-Octavian Duliu, Andrew Reeves, Ilija Hristovski, Amita Shrestha, Florian Moll, and Christian Fuchs. Optical ground station oberpfaffenhofen next generation: first satellite link tests with 80 cm telescope and AO system. In *Proceedings of 2023 IEEE International Conference on Space Optical Systems and Applications (ICSOS 2023)*. ICSOS, 2023.
- [12] Benjamin Rödiger and Christopher Schmidt. In-orbit demonstration of the world's smallest laser communication terminal: OSIRIS4CubeSat/CubeLCT. In Proceedings of Small Satellites Systems and Services Symposium (4S 2024), volume 13546, pages 166– 180. SPIE, 2025.
- [13] FreeRTOS real-time operating system for microcontrollers and small microprocessors. https://freertos.org [Online; accessed 2024-09-20].
- [14] JerryScript a lightweight and embeddable JavaScript engine for IoT devices. https://jerryscript.net [Online; accessed 2024-09-12].
- [15] Lisa Elsner, Timon Petermann, Maximilian von Arnim, and Klaus Schilling. Pre-flight verification of the CubeSat attitude control system for the QUBE

IAC-25,B2,IPB,17,x9948 Page 15 of 16

- mission. In *Proceedings of Small Satellites Systems and Services Symposium (4S 2024)*, volume 13546, pages 1793–1803. SPIE, 2025.
- [16] Lisa Elsner, Johannes Dauner, Benedikt Schmidt, Timon Petermann, Malavika Unnikrishnan, René Rüddenklau, et al. Beacon-enhanced attitude control using optical communication terminals: Design and validation in the QUBE mission. In Proceedings of Workshop on Control Aspects of Multi-Satellite Systems (CAMSAT), in press. IFAC, 2025.
- [17] Timon Petermann, Eric Jäger, Lisa Elsner, Dominik Pearson, Guido Dietl, and Klaus Schilling. A distributed hardware-in-the-loop testbed for attitude control of small communication satellites. In Proceedings of IEEE Space Hardware and Radio Conference (SHaRC), pages 8–11, 2025.
- [18] Timon Petermann, Vijay Nagalingesh, Tom Geiger, Lisa Elsner, Oliver Ruf, and Klaus Schilling. Precision and scalability: Optimizing attitude control testing for reliable multi-satellite systems. In Proceedings of Workshop on Control Aspects of Multi-Satellite Systems (CAMSAT), in press. IFAC, 2025.
- [19] René Rüddenklau, Benjamin Rödiger, Christian Roubal, Christopher Schmidt, and Florian Moll. Vibration load compliance of a miniaturized cubesat quantum communication terminal. *Journal of Vibration and Control*, 2025.
- [20] Martin Hutterer, Michael Auer, Adomas Baliuka, Oemer Bayraktar, Peter Freiwang, Marcell Gall, et al. Qube-II-quantum key distribution with a cubesat. In Proceedings of the 73rd International Astronautical Congress, IAC 2022, 2022.
- [21] Lisa Elsner, Timon Petermann, Johannes Dauner, Jonas-Julian Jensen, Alexander Kleinschrodt, Ilham Mammadov, et al. Cloud characterization by computed tomography methods using a satellite formation of 10 small satellites for improved climate prediction. *Acta Astronautica*, 236:251–262, 2025.
- [22] Jonas Jensen, Johannes Dauner, Alexander Kleinschrodt, Ilham Mammadov, Prachit Kamble, Lisa Elsner, and Klaus Schilling. Cooperative observations by photogrammetric methods with the TOM satellite formation. In *Proceedings of Small Satellites Systems and Services Symposium (4S 2024)*, volume 13546, pages 1342–1356. SPIE, 2025.

IAC-25,B2,IPB,17,x9948 Page 16 of 16